Clays and Clay Minerals, 1973, Vol. 21, pp. 1–7. Pergamon Press. Printed in Great Britain

CHLORITE EXAMINATION BY ULTRAMICROTOMY AND HIGH RESOLUTION ELECTRON MICROSCOPY

J. L. BROWN
Analytical Instrumentation Laboratories, Engineering Experiment Station, Georgia Institute of Technology, Atlanta, Georgia 30332 U.S.A.

and

M. L. JACKSON
Department of Soil Science, University of Wisconsin Madison, Wisconsin 53706, U.S.A.

(*Received* 8 *May* 1972)

Abstract—Mafic chlorite from Benton, Arkansas was comminuted by rotary blending of a suspension, and the $-2\,\mu$m fraction separated by sedimentation in H_2O. Droplets of suspension of the $<2\,\mu$m fraction were dried on a layer of Epoxy resin and then additional Epoxy was added and heat-cured at 48°C to form a resin sandwich. Cross-sections of 600–900 Å thickness were cut on a Reichert automated ultramicrotome. The sections were collected on standard electron microscope specimen screens, reinforced by vacuum evaporated *C* and examined by transmission electron microscopy (TEM). The Phillips EM 200 electron microscope was equipped with a "microgun" source to minimize heating of the specimen and to improve contrast and high resolution (HREM). Images of the (001) chlorite crystallographic planes spaced at 13·9 Å intervals were visible on many of the particle sections. Imaging of the planes depended upon their being nearly parallel to the electron beam (within 0° 10′) and therefore, many particles which had other orientations did not show the 13·9 Å image. Micrographs made before appreciable irradiation by the electron beam revealed images of fringes corresponding to the 7·22 Å (002) spacing of chlorite. Loss of the 7·22 Å fringes and reinforcement of those at 13·9 Å resulted from heating of the chlorite in the electron beam. This behavior is analogous to the well-known crystallographic effects of heating chlorite at 550–760°C.

INTRODUCTION

THE INTERLAYER surfaces of 2:1 phyllosilicates are the sites for intercalation not only of hydrated exchangeable cations but also of hydroxy–metal layers such as those of Fe, Al, and Mg, for which chlorite (Pauling, 1930) is a model mineral. These interlayer configurations are important in cation exchange of radioactive and other ions (Rich, 1968; Syers *et al.*, 1972) and other clay transformations (Jackson, 1963, 1965). Direct photography of ultramicrotomed sections of the crystals examined by high resolution electron microscopy (HREM) has revealed the configuration of the phyllosilicate layers of chrysotile (Yada, 1967) and muscovite (Brown and Rich, 1968). The pyridine intercalated complex of tantalum disulfide (TaS_2) has similarly been photographed (Fernández-Morán *et al.*, 1971).

Margins of montmorillonite particles showed scrolled portions in which the layer intervals were observed edge-on as paralled fringes at 10 Å (Barclay and Thompson, 1969) and 18–40 Å with organic complexes (Suito *et al.*, 1969). Imogolite fiber cross-sections were observed as thin cylinders about 19 Å in dia. in ultramicrotomed sections (Wada *et al.*, 1970). In electron microscope studies of replicas of ferruginous interlayer coatings of micaceous vermiculite (Roth *et al.*, 1967), chlorite was included as a control. The chlorite was ultramicrotomed and direct photographs made of the (001) atomic planes (Brown and Jackson, 1970) by high resolution electron microscopy (UM-HREM) in the present study.

METHOD

A mafic chlorite from Benton, Arkansas (courtesy of S. L. Chapman) was ground in suspension in distilled water with a high speed rotary blender. A suspension of the particle size fraction less than 2 μm equivalent spherical dia. was separated by centrifugation. The sample gave a sharp 14·4 Å basal X-ray diffraction peak and higher integral order peaks for chlorite.

Droplets of the chlorite suspension in water were dried on a cured Epoxy (Araldite 6005 from Cargille Sons, 194 Second Ave., Little Falls, NJ) layer to obtain parallel orientation of the clay particles. The position of the clay coated area was

https://doi.org/10.1346/CCMN.1973.0210102 Published online by Cambridge University Press

circled with India ink to facilitate locating the areas for ultramicrotoming. Additional Epoxy solution was then added and heat cured at 48°C overnight to form an Epoxy sandwich (Brown and Rich, 1968). A small block was sawed from the Epoxy, suitably shaped by filing to center the ink marks, then sectioned by means of a Reichert OmU2 ultramicrotome (Wm. J. Hacker and Co., Inc., P.O. Box 646, West Caldwell, NJ) with a diamond knife. The section was made perpendicularly across the sediment plane so as to cut through the flat faces of the platy particles. The particle platelets and (001) crystal planes in the section thus were approximately normal to the section surface. The thin sections were 600–900 Å thickness, as judged from the Sorvall (Norwalk, CT., 96852) color chart for reflected light. The thin sections were collected from the water-filled boat by touching them with the flat surface of a standard electron microscope grid previously coated with 0·1 per cent bovine albumin (Armour Pharmaceutical Co., Kankakee, IL) and dried. The specimen was dried in an air stream and then strengthened with a very thin layer of *C* (about 100 Å thick) by vacuum evaporation, and examined by transmission electron microscopy (TEM). The Philips EM200 electron microscope was equipped with a "microgun" source to minimize heating of the specimen and to improve contrast and resolution. The accelerating voltage of 100 kV gave an effective electron beam wavelength of 0·037 Å. A 50 μm back focal plane objective aperture was employed, with which the angular aperture of the microscope is sufficient to pass Bragg reflections from crystal spacings as close as 4 Å. Eastman P426 35-mm film was used for the electron micrographs.

RESULTS AND DISCUSSION

Intermediate magnification

The sectioned chlorite platelets distributed in the Epoxy resin are visible (Fig. 1a) at intermediate magnification. During sectioning, the Epoxy tears in places (Fig. 1a) and the clay platelets sometimes fall out. The evaporated carbon film helps to prevent this. The carbon film is essential to conduct away the electrostatic charge that tends to build up on the particles in the electron beam. This keeps the Epoxy film mount intact during the examination in the electron microscope. Without the carbon layer, the Epoxy film quickly ruptures. Larger than 2 μm phyllosilicate particles tend to be torn from the section by the diamond knife instead of being cut. Particles much smaller than 1 μm tend to cake and not accept Epoxy resin between the individual particles. Thus, such particles do not remain securely anchored in the cured resin so as to be sectioned.

High magnification

Calibration of the electron microscope magnification (to an accuracy within $\pm 1\%$), based on a germanium-shadowed carbon replica of a diffraction grating (21,600 lines per cm), shows the fringe-to-fringe distance of the HREM images to represent a 13·9 Å spacing (Figs. 1b, c) in many of the outlines of the sectioned particles. This corresponds to the (001) X-ray diffraction peak of chlorite, representing the repeat interval of the 2 : 1 phyllosilicate crystallographic layers.

When rapid photomicrography of the specimen was carried out, so as to minimize the exposure of the crystal in the intense electron beam required for imaging at high magnification, fringes were observed (Figs. 2a, b), spaced at 7·22 Å, the (002) X-ray diffraction peak of unheated chlorite.

The planes of atoms in crystals diffract (scatter) electrons in much the same way that they diffract X-rays. However, the electrons are diffracted by Rutherford interactions with the electric fields within the atom, whereas the X-rays are scattered by the electron clouds surrounding the atomic nuclei. As a result, HREM imaging can reveal crystal defects or configurations involving successive individual clay layers (for example, Yada, 1967). Since the electron wavelengths used are much shorter than the X-ray wavelengths ordinarily used for crystal diffraction study, the values for diffraction angles (θ, in the Bragg equation, $n\lambda = 2d \sin \theta$) are sufficiently small to be subtended in the microscope aperture. The 14 Å (001) and 7 Å (002) diffraction angles for chlorite are only small fractions of a degree (4′ 30″ and 8′ 57″, respectively). To form the phase contrast fringe images (Figs. 1b, c; 2a, b), the incident electron beam must have these diffraction angles with respect to the diffracting planes in the crystal. Also, the objective aperture must be large enough to pass the diffracted beam since it is necessary, in accordance with the Abbe theory, to combine optically the zero order and at least the first order diffraction beam in the electron image plane (Thomas, 1962, p. 52). Because of spherical aberration in the objective lens of the electron microscope, only those diffracted beams near the objective axis can be successfully used for imaging; otherwise the phase conditions in the image plane cause contrast to be lost.

Many particles (e.g. Fig. 1c, arrow) having other tilt angles do not show the (001) and/or (002) fringes within the usual amplitude contrast TEM image. Amplitude contrast is produced by the back-focal-plane objective aperture and includes both mass–thickness and diffraction contrast. For essentially amorphous mineral and most resin materials, the short range order of individual

https://doi.org/10.1346/CCMN.1973.0210102 Published online by Cambridge University Press

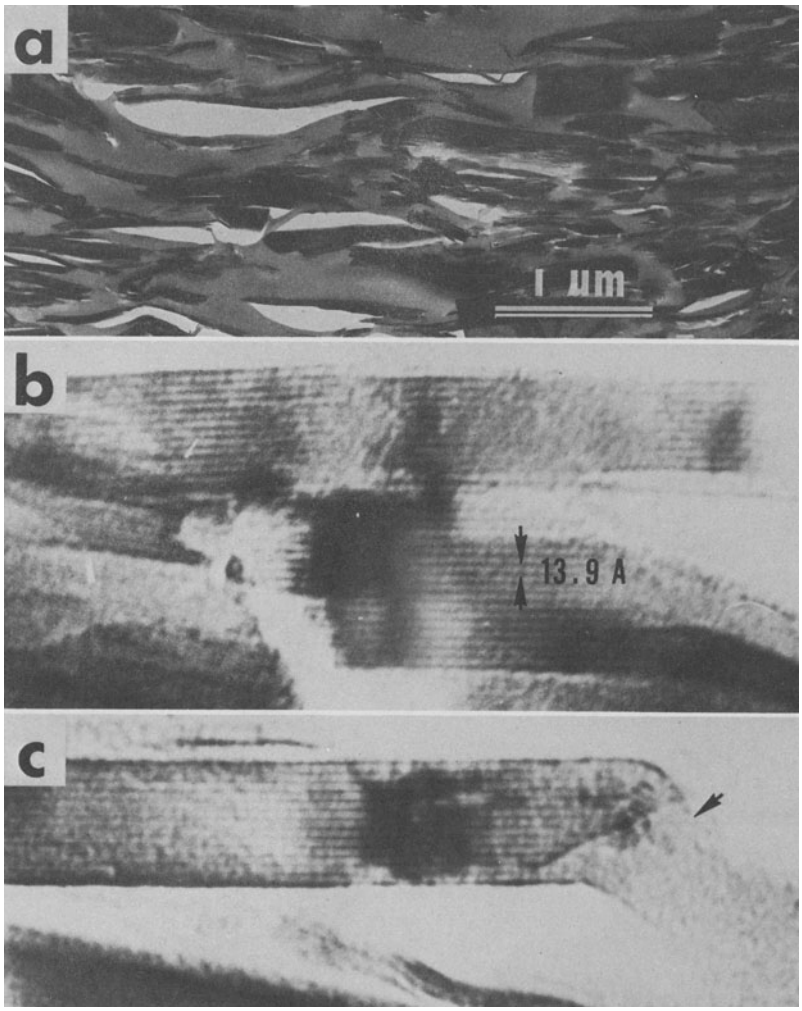


Fig. 1. Transmission electron micrograph of chlorite ($\ll 2\ \mu$m) set in Epoxy plastic and thin-sectioned by a diamond-knife ultramicrotome (a) at intermediate magnification, showing some torn areas in the Epoxy; (b) at high magnification, showing 13·9 Å crystallographic spacings by phase contrast imaging; (c) same, with an area (arrow) not in proper position to show a phase contrast image.

organizational units is smaller than the resolution of the microscope. For such cases, the TEM contrast in the image is dependent solely on mass thickness differences; for example, low-mass Epoxy versus clay particles (Fig. 1a) or particles at non-diffracting tilt angles (Fig. 1c, arrow).

For longer range crystalline order, as in the chlorite sections examined (Figs. 1b, c; 2a, b, c, d), the diffraction angles are small enough to give phase contrast images in the electron microscope. The HREM technique gave superlattice fringes corresponding to 100 Å in Yu Yen Stone (antigorite) crystals (Brindley *et al.*, 1958). Interestingly, the 100 Å fringes of antigorite in one case (their Fig. 1b) are interspersed with faint fringes at 50 Å.

Phase changes (PC) cause light and dark zones in the chlorite images (PC, Fig. 2b, and left of center in Fig. 2d). These zones were also noted in micas (Brown and Rich, 1968, PC in their Fig. 1).

Dark spotty (mottled) areas in the chlorite sections (Fig. 1 and 2) are extinction contours caused by diffraction contrast in which many of the diffracted beams are intercepted by the objective

https://doi.org/10.1346/CCMN.1973.0210102 Published online by Cambridge University Press

aperture and their contribution to the final image is decreased. These effects also appeared as mottling in micaceous vermiculite (Raman and Jackson, 1964).

Crystal damage in the electron beam

The 7·22 Å fringes (Figs. 2b, d) of the chlorite were absent in most of the electron micrographs and were detected only when the photographs were made very rapidly in a given specimen area, by the through-focus technique. This relationship was attributed to crystal damage (dehydroxylation of the hydroxyl interlayers of the chlorite) by the intense electron beam necessary for imaging at high magnification, rather than to a change in the angle of repose of the crystal section. After a short exposure to heat in the electron beam, the electron diffraction leading to the electron optical image formation revealed only 13·9 Å fringes (Figs. 1b, c). In an analogous way, loss of the 7·3 Å fringes from chrysotile and change "to the amorphous state" occurred (Yada, 1967, p. 705) as a result of crystal damage by the electron beam irradiation. Crystal damage, concentrated in

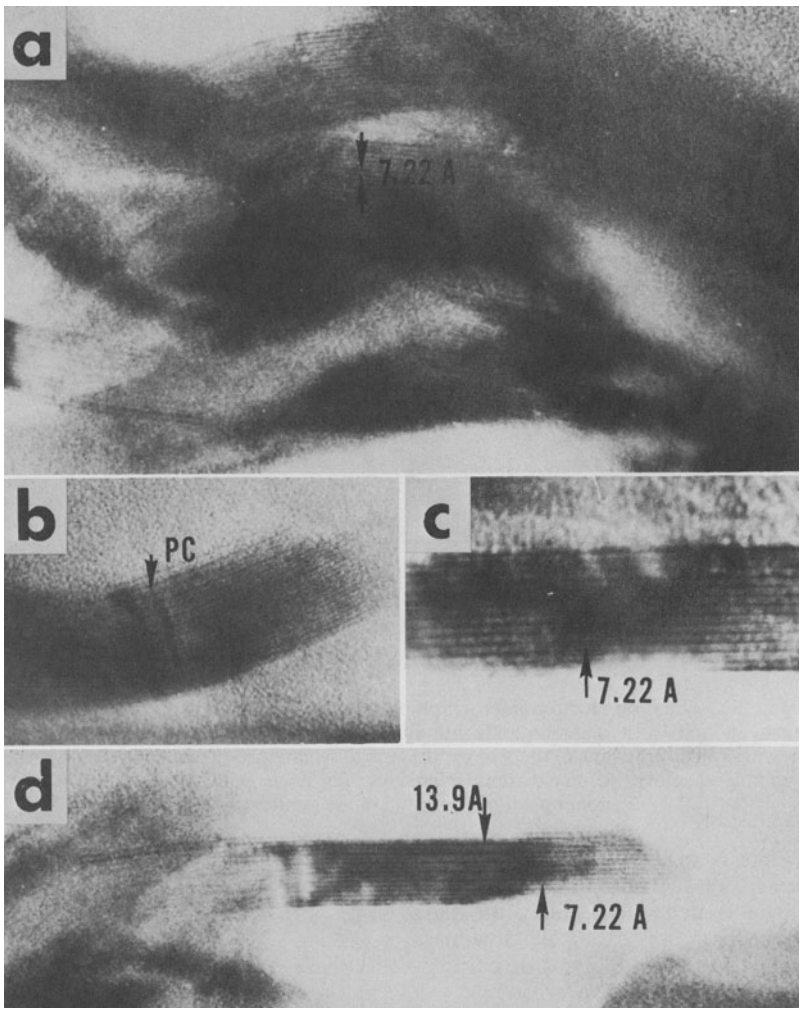


Fig. 2. Transmission electron micrograph of chlorite sections taken rapidly with through-focus technique to minimize specimen heatings (a) showing 7·22 Å spacing; (b) same, with phase change fringes (PC); (c and d) same with areas of 7·22 and 13·9 Å spacings in different parts of the same crystal.

https://doi.org/10.1346/CCMN.1973.0210102 Published online by Cambridge University Press

one part of the crystal (owing to compositional differences or chance) could contribute to difference in resolution of the 7·22 Å fringes in different parts of the crystal. The disruption by heating of a chlorite mineral in the electron beam is analogous to the effect of furnace heating, which causes the well-known loss of 7·22 Å X-ray diffraction peak of chlorite and reinforcement of a 14·1 Å X-ray diffraction peak after 600°C and a 13·9 Å peak after 760°C (Brindley, 1961, p. 253; Alexiades and Jackson, 1967).

Other electron optical interpretations must be considered, since the Bragg angles involved are close to the periphery of the aperture of the microscope. First, the electron optics for the 7·22 Å fringes are more difficult to obtain over the whole sectioned area than those for the 13·9 Å fringes because the permissible angular deviation from Bragg conditions is more critical in the former case (Yada, 1967, p. 707). A slightly different orientation (slight warping) of a portion of the chlorite section might reveal the 13·9 Å (smaller angle) without showing the 7·22 Å (larger angle) fringes. One part of the crystal could remain oriented at a Bragg angle for (002) 7·22 Å fringes and the other for (001) 13·9 Å fringes (Figs. 2c, d). If this effect, however, contributed to resolution of fewer 7·22 Å fringes in the electron micrographs than 13·9 Å fringes, the (001) should have remained at the 14·4 Å spacing of unheated chlorite.

Second, the diffraction of electrons depends heavily upon the atomic number of the chemical elements in the crystal. Scattering by heavy atoms through dynamical diffraction (Heidenreich, 1964, p. 302) causes a phase change in the wave front of the electron beam which could create corresponding interference (phase contrast) effects in the image plane. The heavier atoms, particularly Fe in 6-fold coordination in the mafic chlorite, are particularly effective in this way. A higher Fe concentration either in 2 : 1 layers or in hydroxyl sheets between layers, by dynamical diffraction, could make the 13·9 Å fringe intensity greater than that of the 7·22 Å fringe. The 7·22 Å fringes from an area of the same crystal which shows only the 13·9 Å fringes in other areas (Figs. 2c, d) might, therefore, be attributed in part to appropriate phase shifts resulting from a mosaic of varying elemental composition sequences of octahedral cation sheets in layers and interlayers.

Thickness and crystal perfection of the chlorite particles

A large proportion of the chlorite particles (< 2 μm fraction) are on the order of 150–200 Å thick (Figs. 1 and 2). Since the X-ray diffraction peaks at 14·4 and 7·2 Å for this sample were very intense (data not shown herein), the images (Figs. 1 and 2) show that as few as 10–20 (001) crystallographic units are ample for development of sharp X-ray diffraction maxima. The question of the necessary number of planes for sharp X-ray diffraction peaks still arises frequently, although Scherrer calculated the presently observed number a half century ago.

No distortion of the chlorite crystal is observable on the outside boundary of the images (Figs. 1 and 2), indicating that no short range structural damage at the edges was created by surface tension effects or by the mechanical comminution process. No mass contrast image extended beyond the diffraction contrast image. The question as to whether outermost "disturbed" layers and/or edges would be created by comminution in a high speed rotary blender is thus settled negatively for this chlorite.

CONCLUSIONS

1. High resolution electron microscopy of ultramicrotomed sections, made normal to the basal planes of the chlorite, revealed phase contrast electron optical image fringes corresponding to the 7·22 Å (002) diffraction peak of chlorite before heating and to a 13·9 Å (001) peak after heating.

2. Many more crystal specimens were seen with 13·9 Å fringes than with 7·22 Å fringes. Most crystals showed greater intensities of 13·9 Å fringes than of 7·22 Å fringes. A few crystals showed long sequences of equal-intensity fringes at 7·22 Å when the electron micrographs were made rapidly with the through-focus technique. The 7·22 Å fringes were subject to loss during a few minutes of exposure in the intense electron beam of the microscope operated at 100 kV, leaving reinforced 13·9 Å images, as for chlorite furnace-heated at 760°C.

3. Single plate particles of < 2 μm equivalent spherical dia. were frequently of 10–20 unit cells (each of 14 Å) thickness. This size fraction gave very sharp X-ray diffraction peaks in separate studies.

4. No evidence of a "disturbed" layer, or coatings of short range order only, occurred in the outermost layer or at the ends of the chlorite particles, which had been comminuted by high-speed rotary blending of a suspension.

Acknowledgements—This cooperative research was supported in part by the College of Agricultural and Life Sciences, University of Wisconsin, under project 1336, in part by the Analytical Instrumentation Laboratories, Engineering Experiment Station, Georgia Institute of Technology, and in part by the Ecological Sciences Branch Division of Biomedical and Environmental Research, United States Atomic Energy commission

https://doi.org/10.1346/CCMN.1973.0210102 Published online by Cambridge University Press

Contract AT(11-1)-1515-Jackson (paper COO-1515-25) and the National Science Foundation grant GP1108-Jackson. Gratitude is expressed to Mr. S. Y. Lee for assistance with the printing and mounting of the electron micrographs.

REFERENCES

Alexiades, C. A. and Jackson, M. L. (1967) Chlorite determination in clays of soils and mineral deposits: *Amer. Mineral.* **52**, 1855–1873.

Barclay, L. M. and Thompson, D. W. (1969) Electron microscopy of sodium montmorillonite: *Nature* **222**, 263.

Brindley, G. W. (1961) Chlorite minerals. In *X-ray Identification and Crystal Structures of Clay Minerals* (Edited by G. Brown), Chap. 6, pp. 242–296. The Mineralogical Society, London.

Brindley, G. W., Comer, J. J., Uyeda, R. and Zussman, J. (1958) Electron-optical observations with crystals of antigorite: *Acta Crystallog* **11**, 99–102.

Brown, J. L. and Jackson, M. L. (1970) Chlorite examination by ultramicrotomy and high resolution electron microscopy: *Abstracts, 19th Clay Miner. Conf.*, FL, p. 13.

Brown, J. L. and Rich, C. I. (1968) High resolution electron microscopy of muscovite: *Science* **161**, 1135–1137.

Fernández-Morán, J., Ohstuki, M., Hibino, A. and Hough, C. (1971) Electron Microscopy and diffraction of layered, superconducting intercalation complexes: *Science* **174**, 498–500.

Heidenreich, R. (1964) *Fundamentals of Transmission Electron Microscopy*: Interscience, New York.

Jackson, M. L. (1963) Interlayering of expansible layer silicates in soils by chemical weathering: *Clays and Clay Minerals* **11**, 29–46.

Jackson, M. L. (1965) Clay transformations in soil genesis during the Quaternary: *Soil Sci.* **99**, 15–22.

Pauling, L. (1930) Structure of chlorites: *Proc. Nat. Acad. Sci.* (Wash) **10**, 692–694.

Raman, K. V. V. and Jackson, M. L. (1964) Vermiculite surface morphology: *Clays and Clay Minerals* **12**, 423–429.

Rich, C. I. (1968) Hydroxy interlayers in expansible layer silicates: *Clays and Clay Minerals* **16**, 15–30.

Roth, C. B., Jackson, M. L., de Villiers, J. M. and Volk, V. V. (1967) Surface colloids on micaceous vermiculite. In *Soil Chemistry and Soil Fertility* (Edited by G. V. Jacks), pp. 217–221 *Trans. Comm. II and IV, Intl. Soc. Soil Sci.*, Aberdeen. Intl. Soc. Soil Sci. publ.

Suito, E., Arakawa, M. and Yoshida, T. (1969) Electron microscopic observation of the layer of organo-montmorillonite: *Proc. 3rd Intl. Clay Conf.* Tokyo, 1, 757–763.

Syers, J. K., Mokma, D. L., Jackson, M. L., Dolcater, D. L. and Rex, R. W. (1972) Mineralogical composition and cesium-137 retention properties of continental aerosolic dusts: *Soil Sci.* **113** 116–123.

Thomas, G. (1962) *Transmission Electron Microscopy of Metals*: Wiley, New York.

Wada, K., Yoshinaga, N., Yotsumoto, H., Ibe, K. and Aida, S. (1970) High resolution electron micrographs of imogolite: *Clay Minerals* **8**, 487–489.

Yada, K. (1967) Study of chrysotile asbestos by a high resolution electron microscope: *Acta Crystalog.* **23**, 704–707.

Résumé—Une chlorite mafique de Benton, Arkansas a été pulvérisée par broyage d'une suspension dans un homogéniseur rotatif, et la fraction $< 2\ \mu$m a été séparée par sédimentation dans l'eau. Des gouttelettes de la suspension de la fraction $< 2\ \mu$m étaient désséchées sur une couche de résine Epoxy; puis une couche supplémentaire d'Epoxy était ajouée; l'ensemble était enfin chauffé à 48°C pour former un sandwich entre les deux couches de résine. Des tranches de 600 à 900 Å d'épaisseur étaient découpées avec un ultramicrotome automatique de Reichert. Les coupes étaient déposées sur les grilles porte-échantillon standard pour microscope électronique, renforcées par évaporation sous vide de C puis examinées par microscopie électronique de transmission (TEM). Le microscope électronique Philips EM 200 utilisé, était muni d'une source "microgun" afin de minimiser l'échauffement de l'échantillon et d'améliorer le contraste et la haute résolution (HREM). Les images des plans cristallographiques 001 de la chlorite, espacés par des intervalles de 13, 9 Å sont visibles sur de nombreuses coupes. L'obtention des images des plans n'est possible que si ces plans sont à très peu près parallèles au faisceau d'élections (angle admissible 0° 10′) et, de la sorte, de nombreuses particules qui ont d'autres orientations ne montrent pas l'image à 13,9 Å. Les micrographies effectuées avant que l'échantillon n'ait reçu une irradiation électronique appréciable révèlent l'image de franges correspondant à l'espacement 002 de la chlorite à 7,22 Å. La disparition des franges à 7,22 Å et le renforcement de celles à 13,9 Å est dû au chauffage de la chlorite par le faisceau d'électrons. Ce comportement est analogue aux effets cristallographiques bien connus qui sont observés quand on chauffe la chlorite de 550 à 760°C.

Kurzreferat—Mafisches Chlorit aus Benton, Arkansas, wurde unter drehendem Mischen einer Suspension zerkleinert, und die $\leftarrow 2\mu$ Fraktion wurde durch Absetzung in H_2O abgeschieden. Suspensionströpfchen der $< 2\mu$ Fraktion wurden auf einer Epoxyharzschicht getrocknet, worauf weiteres Epoxyharz hinzugefügt wurde. Nach Warmhärtung bei 48°C entstand ein "Harzsandwich". Es wurden mit Hilfe eines automatischen Reichert Ultra-Mikrotoms Querschnitte von 600 bis 900 Å Dicke hergestellt. Die Schnitte wurden auf normalen Elektronenmikroskop-Trägernetzen gesammelt, durch Aufdampfen von *C* unter Vakuum verstärkt und mit Hilfe eines Durchstrahlungs-Elektronenmikroskops (TEM) geprüft. Das Phillips EM 200 Elektronenmikroskop war mit einer Strahlenrichtquelle

https://doi.org/10.1346/CCMN.1973.0210102 Published online by Cambridge University Press

(microgun) ausgestattet, um Erhitzung der Probe auf ein Mindestmaß einzuschränken und den Kontrast sowie die Auflösung zu verbessern (HREM). Bilder der (001) kristallographischen Ebenen des Chlorits in Abständen von 13,9 Å waren bei vielen der Teilchenschnitte sichtbar. Die Abbildung der Ebenen setzte voraus, daß sie nahezu parallel zu dem Elektronenstrahl (innerhalb von 0°10′) verliegen, und viele Teilchen mit anderen Orientierungen ergaben das 13,9 Å Bild nicht. Mikrogramme, die ausgeführt wurden, bevor erhebliche Bestrahlung durch den Elektronenstrahl stattfand, wiesen Säume auf, die der 7,22 Å (002) Struktur des Chlorits entsprachen. Erhitzung des Chlorits im Elektronenstrahl führte zu Verlust der 7,22 Å Säume und Verstärkung der 13,9 Å Säume. Dieses Verhalten ist den bekannten kristallographischen Auswirkungen der Erhitzung von Chlorit auf 550 bis 760°C analog.

Резюме — Мафический хлорит, найденный в Бентоне, Арканзас, измельчался путем вращательного перемешивания суспензии и частицы размером 2 μm отделялись седиментацией в H_2O. Капельки суспензии <2 μm сушились на слое эпоксидной смолы, сверху клали еще один слой эпокси и сушили при температуре 48°C для получения «сандвича», затем этот блок рассекался на автоматическом ультрамикротоме Рейхерта на срезы толщиной 600–900 Å. Эти срезы собрали на предметное стекло стандартного электронного микроскопа, усилили выпаренным под вакуумом C и рассматривали под просвечивающим электронным микроскопом. Электронный микроскоп EM 200 Phillips оснащен «микропульверизатором» для понижения нагрева образца и для улучшения контраста и разрешающей способности. Изображения кристаллографических плоскостей (001), расположенных с интервалами 13,9 Å видимы на сечениях частиц. Получили изображения только тех плоскостей, которые были расположены почти что параллельно к электронному пучку (в пределах 0° 10′) и, поэтому многие частицы имеющие другую ориентацию не были видны на изображении 13,9 Å. Микроснимки электронным пучком показали изображения полос 7,22 Å, а усиление их в 13,9 Å получилось в результате подогревания хлорита в электронном пучке. Это поведение аналогично хорошо известным кристаллографическим эффектам нагретого до 550–760°C хлорита.

https://doi.org/10.1346/CCMN.1973.0210102 Published online by Cambridge University Press